toxics

MDPI

Article

Formulation-Associated Pro-Oxidative and Pro-Inflammatory Activation of Adherent and Nonadherent THP-1 Monocytic Cells Induced by E-Cigarette Aerosols

Katarzyna Milewska [1], Piotr Szoka [1], Joanna Roslan [2] and Adam Holownia [1,*]

[1] Department of Pharmacology, Medical University of Bialystok, Mickiewicza 2c, 15-222 Bialystok, Poland; katarzyna.milewska@umb.edu.pl (K.M.); piotr.szoka@umb.edu.pl (P.S.)
[2] Department of Obstetrics and Gynaecology, Sniadeckiego Voivodeship Hospital, M. Curie-Skłodowskiej 26, 15-950 Białystok, Poland
* Correspondence: adam.holownia@umb.edu.pl; Tel.: +48-85-7485570

Abstract

Electronic cigarettes are widely promoted as a less harmful alternative to conventional cigarettes, but their cellular effects remain incompletely defined and may vary by flavouring composition. This exploratory screening study examined the effects of four flavoured e-cigarette aerosols, cigarette smoke, and nicotine on human THP-1 monocytic cells, focusing on cytotoxicity, oxidative stress, inflammatory activation, adhesion, and phagocytic function. Cells were exposed for 24 h to conditioned media containing 0.1 mg/mL nicotine; generated using a standardised puffing protocol; and then analysed by microscopy, trypan blue exclusion, flow cytometry, and dual-fluorescence scatterplot analysis. Cigarette smoke-conditioned medium produced the greatest acute toxicity, significantly increasing cell death, membrane damage, and DNA fragmentation. In contrast, the tested e-cigarette aerosol-conditioned media and nicotine alone produced little overt cytotoxicity under the same experimental conditions. However, e-cigarette exposures increased cell adhesion and were associated with formulation- and cell subpopulation-dependent changes in CD11a, CD11b, and CD54 expression. E-cigarettes increased intracellular DCF-associated oxidative fluorescence and TNF-α expression, with the watermelon and strawberry formulations producing the strongest responses. Nicotine alone did not significantly alter the principal oxidative and intracellular TNFα endpoints relative to the corresponding controls. Numerical differences between adherent and nonadherent fractions remain exploratory and do not establish opposing biological effects. These findings indicate that aerosol components other than nicotine may contribute substantially to biological activity and that the response may be bimodal. Phagocytosis was reduced in selected groups, suggesting that some exposures may impair this cellular function. Bivariate fluorescence analysis revealed exposure-dependent differences in the relationship between DCF-associated oxidative fluorescence and TNF-α expression, with cigarette smoke producing the most pronounced disruption. Overall, these findings support the potential utility of bivariate fluorescence analysis as a complementary in vitro approach for detecting and comparing oxidative and inflammatory cellular responses to different e-cigarette aerosols.

Keywords: e-cigarettes; inflammation; THP-1 cells; TNFα; DCF-associated oxidative fluorescence

Check for updates

Academic Editor: Jian Sun

Received: 21 October 2026
Revised: 11 November 2026
Accepted: 25 November 2026
Published: 28 November 2026

Copyright: © 2026 by the authors. Licensee MDPI, Basel, Switzerland. This article is an open access article distributed under the terms and conditions of the Creative Commons Attribution (CC BY) license.

1. Introduction

Cigarette smoking remains a major cause of preventable morbidity and mortality worldwide, contributing substantially to chronic obstructive pulmonary disease, cardiovascular disease, and malignancies of the lung and other organs [1,2]. Although nicotine (N) dependence continues to hinder smoking cessation, electronic cigarettes (ECs) have emerged as alternative N delivery systems that may reduce exposure to certain toxicants relative to conventional cigarettes. However, ECs are not without risk, particularly among dual users, and their toxicological profile remains incompletely characterised [3,4].

The rapid expansion of the EC market has introduced substantial heterogeneity in device design, liquid composition, and flavouring agents, thereby complicating both biological interpretation and regulatory evaluation. Existing studies suggest that EC aerosols may induce oxidative stress [4,5], activate inflammatory pathways [6,7], and trigger cell death [8]; nevertheless, the reported effects remain inconsistent, largely because of differences in experimental conditions and aerosol composition. This variability underscores the need for standardised experimental models that generate reproducible, comparable data across products and studies.

Monocyte/macrophage-based systems, including the THP-1 cell line, represent a useful platform for the early assessment of EC-associated toxicity. Derived from human monocytes, THP-1 cells are widely used to model macrophage-related inflammatory responses and innate immune function [9]. These cells permit direct evaluation of the effects of aerosol constituents such as N, propylene glycol (PG), vegetable glycerin (VG), aldehydes, heavy metals and flavouring products on biologically relevant pathways implicated in lung cancer, sarcoidosis and obstructive lung diseases, including COPD and asthma. Prior work has shown that EC aerosols increase DCF-associated oxidative fluorescence [10–13], activate NF-κB signalling [14], and promote the release of inflammatory mediators [15,16], thereby partly recapitulating key features of smoke-related cellular stress. In our previous studies, EC increased human monocyte adherence, induced modest cytotoxicity and DCF-associated oxidative fluorescence relative to conventional cigarettes, and revealed marked heterogeneity in cellular responses, suggesting subpopulation-specific effects. Adherent monocytes exposed ex vivo to EC exhibited increased expression of integrins CD11a and CD11b, intracellular adhesion molecules (ICAM-1; CD54), TNFα, and DCF-associated oxidative fluorescence compared with nonadherent cells, and these effects were further amplified by EC [17]. Moreover, dual-fluorescence flow cytometry demonstrated a taste-specific shift toward a pro-inflammatory and pro-oxidative phenotype in a subset of cells, including macrophage M1-like CD68 expression in adherent subpopulations [17]. A similar bivariate fluorescence approach previously revealed formulation-dependent differences in oxidative and inflammatory responses in A549 epithelial cells, supporting the potential applicability of this analytical strategy across different cellular models [18].

Collectively, these findings support the concept that EC exposure may induce formulation-associated inflammation through selective monocyte activation [19]. Accordingly, there is a pressing need for sensitive experimental models to characterise different EC products and their biological effects. The present study applies joint analysis of DCF-associated oxidative fluorescence and intracellular TNFα-associated fluorescence to operationally separated adherent and nonadherent THP-1 fractions exposed to four commercial EC-aerosol-conditioned media. The exploratory contribution of this study is the integration of these measurements with adhesion-related and functional endpoints.

2. Materials and Methods

2.1. Reagents

Unless otherwise noted, chemical reagents were supplied by Sigma-Aldrich (Poznań, Poland). Cell culture media and reagents were obtained from GIBCO (Thermo Fisher Scientific, Waltham, MA, USA). The fluorescently labelled antibodies used in this study were obtained from Abcam (Cambridgeshire, UK) and Cell Signaling Technology (Danvers, MA, USA).

2.2. Cell Cultures and Treatment

The human monocytic THP-1 cell line (ATCC® TIB202™; Manassas, VA, USA) was used in this study. Cells were cultured in ATCC-formulated RPMI 1640 medium supplemented with 5% fetal calf serum (FCS), 2 mM L-glutamine, 0.05 mM 2-mercaptoethanol, and 100 U/mL penicillin-streptomycin. Cells were maintained at 37 °C in a humidified 5% CO_2 incubator. For specific assays, cells were seeded into 6-well plates (flow cytometry), whereas 12-well plates were used for phagocytosis assays. Cells were subsequently exposed to control or EC-conditioned media for 24 h, as described below. For general experimental procedures, cells were seeded at a density of 0.15×10^6 cells per well and incubated overnight before treatment. For treatment experiments, cells were seeded in 6- or 12-well plates and incubated overnight. Cells were then exposed for 24 h to control medium, cigarette smoke (CS)-conditioned medium, EC aerosol-conditioned medium: EC1 (classic tobacco), EC2 (menthol), EC3 (watermelon), or EC4 (strawberry), or medium supplemented with N. Nonadherent cells were collected by centrifugation; adherent cells were mechanically detached and treated as nonadherent cells, considered as operationally separated culture fractions and not as distinct physiological cell types. Their separation permitted exploratory assessment of response heterogeneity but did not establish distinct physiological macrophage states.

All samples were filtered via a 40 µm cell strainer to remove aggregates, and cells were counted using an inverted phase-contrast microscope combined with a hemocytometer.

Cell Exposure

Conditioned and control media were generated using a standardised puffing protocol via a low-pressure vacuum pump, with the same pressure settings and experimental configuration used for both air, combustible cigarettes, and EC. EC-aerosols were generated from P1 e-liquids (CHIC Sp. z o.o., Ostrzeszow, Poland) containing 12 mg/mL N in four flavour formulations, using 3-s puffs at 10-s intervals to approximate the puffing pattern used for combustible cigarettes. Cigarette smoke-conditioned medium (CS) was generated by drawing smoke from two Marlboro Red cigarettes with the filters removed through the culture medium, with each cigarette consumed over approximately 1 min. The resulting CS-conditioned medium was used as a laboratory smoke comparator rather than as a standardised reference exposure. One combustible cigarette was consumed in approximately 12 puffs. The N concentration in the CS-conditioned medium and EC-conditioned medium was approximately 0.1 mg/mL, as determined by GC-MS. Based on this value, six EC puffs were used to generate EC-conditioned medium with a comparable N concentration. All final samples contained N at an equimolar concentration of 0.1 mg/mL. In the N-only conditioned media, N was added directly from a stock solution to achieve the same molar concentration. All media were sterilised using a 0.22-µm filter and immediately applied to the cultured cells. This approach enabled subsequent experiments to be standardised according to N concentration, allowing nicotine-matched comparisons between CS- and EC-conditioned media.

2.3. Microscopy and Cell Morphology

Following 24 h of exposure to conditioned media, adherent cells and cytospun nonadherent cells were stained with Giemsa-Wright and analysed by light microscopy to determine morphological changes and proliferation indices across experimental groups.

2.4. Assessment of Cell Viability and Hypodiploid DNA Content

Cell viability and DNA damage were assessed using the trypan blue exclusion assay and propidium iodide (PI)-based flow cytometric analysis, respectively. For nonadherent cells, suspensions were harvested, cytospun onto glass slides, and stained; adherent cells were evaluated in situ within culture dishes using inverted light microscopy. Cell viability was calculated as the percentage of trypan blue-negative cells relative to the total number of cells counted. Cell membrane integrity was additionally assessed by measuring lactate dehydrogenase (LDH) release into the culture medium using the Abcam LDH kit (Abcam, Cambridge, UK). Cellular DNA content was assessed by flow cytometry following staining with propidium iodide (PI). PI fluorescence was measured using a CytoFLEX flow cytometer (Beckman Coulter, Warsaw, Poland). DNA-content histograms were analysed using MultiCycle software, version 307 (Phoenix Flow Systems Inc; San Diego, CA, USA.), and the proportion of cells in the hypodiploid pre-G0/G1 (sub-G1) region was quantified.

2.5. Assessment of Intracellular DCF-Associated Oxidative Fluorescence

Intracellular oxidative activity was evaluated using the fluorescent probe DCFDA (2′,7′-dichlorodihydrofluorescein diacetate). Following cellular uptake, intracellular esterases deacetylate non-fluorescent DCFDA to H_2DCF, which is subsequently oxidised to fluorescent DCF, providing an indirect measure of intracellular DCF-associated oxidative fluorescence [20]. DCF fluorescence was measured by flow cytometry and analysed using single-parameter histograms. Increased intracellular DCF-associated oxidative fluorescence was identified by a rightward shift in DCF fluorescence and an increase in mean fluorescence intensity. Assay responsiveness was confirmed using 50 µM tert-butyl hydroperoxide (tBHP) as a positive control, which consistently elicited a pronounced increase in DCF fluorescence.

2.6. Quantification of Cell Adhesion Markers: CD11a, CD11b, and CD54

To minimise non-specific antibody binding, cells were pre-incubated for 30 min at room temperature with a blocking solution containing 5% normal mouse serum, 5% normal rat serum, and 1% Fc Block (eBioscience, San Diego, CA, USA) in PBS. Cells were subsequently stained with fluorescently labelled monoclonal antibodies against CD11a, CD11b, and CD54 or with the corresponding isotype-matched controls (Abcam, Cambridge, UK). After two washes with PBS, the samples were fixed in 0.4% paraformaldehyde and analysed by flow cytometry using a CytoFLEX flow cytometer (Beckman Coulter, Warsaw, Poland). Flow-cytometric data were analysed using Kaluza software (version 2.1.2).

2.7. Quantification of Intracellular TNFα

To assess intracellular TNFα expression, THP-1 cells were fixed in 0.4% paraformaldehyde for 10 min at room temperature and subsequently stained with a PC5.5-conjugated rabbit monoclonal antibody against TNFα (1:200; Cell Signaling Technology, Danvers, MA, USA). Staining was performed for 20 min in the dark in a permeabilisation buffer containing 0.1% Triton X-100 (Sigma-Aldrich, Poznan, Poland) and 1% bovine serum albumin. Cells were subsequently washed, passed through 100-µm cell strainers to remove aggregates, and analysed using a CytoFLEX flow cytometer (Beckman Coulter, Warsaw, Poland), with 5000 events acquired per sample.

2.8. Assessment of Phagocytic Activity

To assess phagocytic activity, THP-1 cells from each experimental group were incubated for 2 h with PE-labelled IgG-coated latex beads (Cayman Phagocytosis Assay Kit; Cayman Chemical, Ann Arbor, MI, USA). Following incubation, cells were washed twice with the appropriate assay buffer to remove unbound beads. Uptake of fluorescent beads was subsequently quantified by flow cytometry using a CytoFLEX flow cytometer (Beckman Coulter, Warsaw, Poland) as described in Cayman's kit [21]. It should be noted that dynamic assessment of phagocytosis and endpoint-specific positive controls were not used.

2.9. Bivariate Analysis of Oxidative Activity and Intracellular TNFα Expression

To evaluate oxidative and inflammatory responses within THP-1 cell subpopulations, intracellular oxidative activity and TNFα expression were assessed in the same cells using bivariate flow-cytometric analysis. Viable cells were first stained with DCFDA to assess intracellular oxidative activity. Following DCFDA staining, cells were washed and fixed in 4% methanol-free formaldehyde for 10 min at room temperature. Fixed cells were subsequently permeabilised and stained with a PC5.5-conjugated rabbit monoclonal antibody against TNFα (1:200; Cell Signaling Technology, Danvers, MA, USA). TNFα staining was performed for 20 min in the dark in a permeabilisation buffer containing 0.1% Triton X-100 and 1% bovine serum albumin. Cells were subsequently washed, passed through 100-µm cell strainers to remove aggregates, and analysed using a CytoFLEX flow cytometer (Beckman Coulter, Warsaw, Poland), with 5000 events acquired per sample. Cell doublets were excluded using 40 µm cell strainers (Sigma-Aldrich, Poznan, Poland) and based on forward-scatter area versus height (FSC-A/FSC-H). DCF and TNFα-associated fluorescence signals were detected in the corresponding green and red fluorescence channels, respectively, and visualised using single-parameter histograms and bivariate density plots. Both fluorophores were bright and clearly separated; therefore, fluorescence minus one (FMO) controls were not considered necessary. Unstained and single-stained controls were sufficient to define the positive and negative populations. Data were analysed using Kaluza software (version 2.1.2) to determine fluorescence intensity, population distribution, and predefined vector-based parameters describing exposure-associated shifts in the bivariate fluorescence plots.

2.10. Statistical Analyses

Statistical analyses were performed to evaluate differences within and between experimental groups. For normalised data expressed relative to a control value of 100% (floating cells), differences from the reference value were assessed using Student's *t*-test. Differences among multiple treatment groups were assessed using one-way analysis of variance (ANOVA), followed by Bonferroni-adjusted post hoc comparisons. All tests were two-sided and $p < 0.05$ was considered statistically significant.

3. Results

3.1. Cytotoxicity, Cell Membrane Damage and Hypodiploid DNA Content

Figure 1A–C show the effect of four EC aerosols, EC1 (classic tobacco), EC2 (menthol), EC3 (watermelon), or EC4 (strawberry), as well as cigarette smoke (CS) and N, on cell viability (A), cell membrane damage (B) and DNA fragmentation (C) in THP-1 cells. Exposure of cells to EC1-EC4 or N for 24 h did not produce significant toxicity to the cell membrane, DNA structure, or overall cell survival, whereas CS exposure generated substantial cytotoxicity across all assays, with approximately 20% of cells dying in each assay. CS significantly increased dead cell numbers (A; $p < 0.01$), cell membrane damage

(B; $p < 0.01$), and DNA damage (C; $p < 0.01$) compared to the control. Compared with N-treated cells, EC1 and EC2 showed significantly higher hypodiploid DNA content ($p < 0.05$).

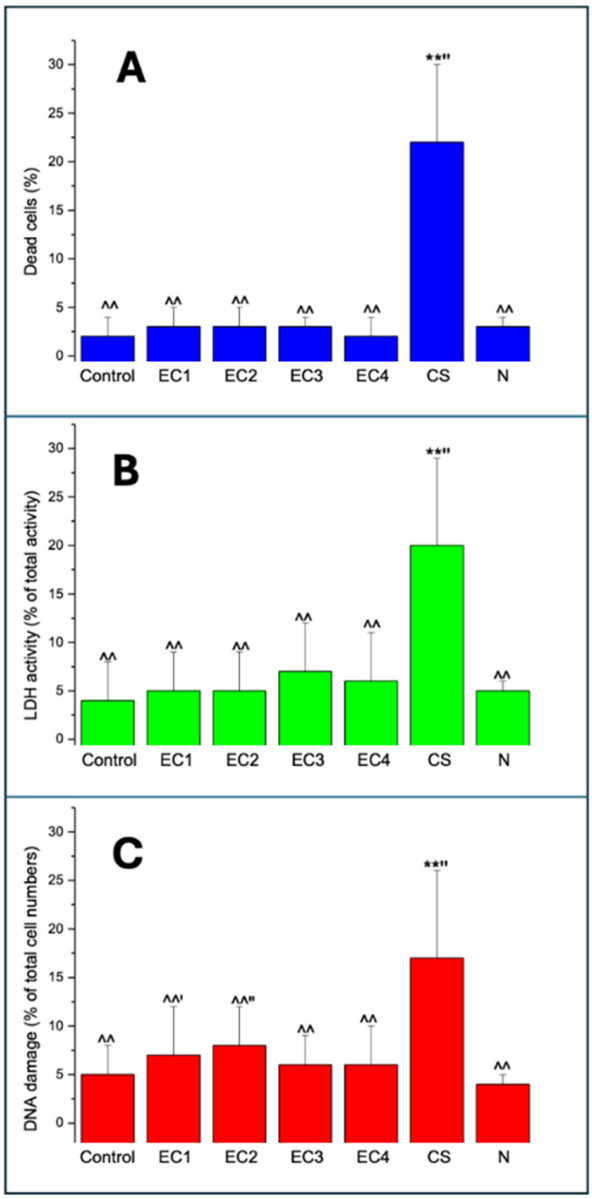


Figure 1. The effect of four electronic cigarette aerosols (EC1 (classic tobacco), EC2 (menthol), EC3 (watermelon), or EC4 (strawberry), cigarette smoke (CS) or nicotine (N) on cell viability (**A**), cell membrane (**B**) and hypodiploid DNA content (**C**) in the monocyte-macrophage cell line THP-1 cells. The EC and CS were prepared as described in Materials and Methods. Cells were kept in EC-, CS- or N-conditioned media for 24 h. Cell viability was tested with the trypan blue exclusion test, cell membrane damage was quantified using released lactate dehydrogenase (LDH), and hypodiploid DNA content was measured using cell cycle-specific DNA fluorescence (propidium iodide staining and flow cytometry). ** $p < 0.01$ for comparisons with the corresponding control cells; ^^ $p < 0.01$ for comparisons with CS-treated cells; ' $p < 0.05$; '' $p < 0.01$ for comparisons with N-treated cells.

3.2. Cytotoxicity, Oxidative Stress, Phagocytosis and Intracellular Inflammation-Related Markers

Table 1 shows the effects of EC1-EC4, CS and N on cell adhesion, integrin CD11a and CD11b expression, intracellular TNFα, DCF-associated oxidative fluorescence and phagocytosis in floating (F) and adherent (A) THP-1 cells exposed for 24 h to electronic cigarette aerosols (EC1-EC4), cigarette smoke (CS) or nicotine (N) as single-endpoint measurements.

Table 1. The effect of electronic cigarette aerosols (EC1-EC4), cigarette smoke (CS) and nicotine (N) on cell adhesion, integrin CD11a, CD11b and CD54 expression, TNFα, DCF-associated oxidative fluorescence and phagocytosis in floating (F) and adherent (A) THP-1 cells. CD11a, CD11b, CD54 and intracellular TNFα were quantified using fluorescent monoclonal antibodies and flow cytometry as described in Materials and Methods. DCF-associated oxidative fluorescence and phagocytosis were assessed using 5-(and-6)-carboxy-2′,7′-dichlorodihydrofluorescein diacetate staining and fluorescent latex beads, respectively, followed by flow-cytometric detection. All values are relative; all control values refer to floating cells, expressed as 100%, from five to six independent experiments.

Cell Adhesion, Integrins, Intracellular Inflammation-Related Markers, DCF-Associated Oxidative Fluorescence and Phagocytosis as Single-Endpoint Measurements							
	Control	EC1	EC2	EC3	EC4	CS	N
Cell adhesion (% of adherent cells)							
	9 ± 4	17 ± 5 *^^′′	21 ± 7 *^^′′	15 ± 6 *^^′′	19 ± 6 *^^′′	3 ± 4	8 ± 5
Integrin CD11a (relative units)							
F	100 ± 17	126 ± 22 *′′	110 ± 23	107 ± 19	109 ± 21	134 ± 28 *′′	103 ± 14
A	131 ± 19 #′′′	145 ± 31 ′′	136 ± 24 ′′	145 ± 32 ′′	144 ± 43 ′′	128 ± 26 ##	99 ± 13 ^^
Integrin CD11b (relative units)							
F	100 ± 13	132 ± 31 *′′	118 ± 25	109 ± 24	123 ± 19′′	131 ± 23 *′′	95 ± 17 ^
A	127 ± 26 #	174 ± 22 **#′′	184 ± 34 **##′′	143 ± 33 **	176 ± 36 **##′′	166 ± 24 **#′′	121 ± 16 #
CD54 (relative units)							
F	100 ± 17	145 ± 19 **^′	134 ± 28 *′	109 ± 21	107 ± 36	109 ± 31	102 ± 15
A	130 ± 24 #	166 ± 34 ′	143 ± 27 ′′	154 ± 27 ##′′	154 ± 33 #′′	146 ± 35 ′′	99 ± 21 ^
TNFα (relative units)							
F	100 ± 18	115 ± 30	139 ± 34 *	141 ± 35 *	138 ± 32 *	145 ± 33 *	87 ± 16 ^^
A	87 ± 26	137 ± 27 **	156 ± 31 **′′	172 ± 40 *′′	164 ± 46 **′′	221 ± 54 **′′	108 ± 22 ^^
DCF-associated oxidative fluorescence (relative units)							
F	100 ± 22	141 ± 38 *^^	139 ± 22 *^^	164 ± 41 **^^	149 ± 42 *^^	313 ± 63 **′′′	89 ± 27 ^^
A	91 ± 27	158 ± 35 **^^	174 ± 47 **^^′′	197 ± 44 **^^′′	179 ** ± 48 ^^′′	362 ± 58 **′′	121 ± 26 ^^
Phagocytosis (relative units)							
F	100 ± 24	84 ± 35	79 ± 28	69 ± 29	59 ± 26 *	49 ± 33 *	71 ± 13 *
A	91 ± 21	75 ± 29	77 ± 39	77 ± 28	62 ± 37	70 ± 35	72 ± 14

* $p < 0.05$; ** $p < 0.01$ for comparisons with the corresponding control cells; # $p < 0.05$; ## $p < 0.01$ for comparisons between control floating cells; ^ $p < 0.05$; ^^ $p < 0.01$ for comparisons with CS-treated cells; ′ $p < 0.05$; ′′ $p < 0.01$ for comparisons with N-treated cells.

Cell adhesion rose from 9% in control cells to 17% with EC1 ($p < 0.05$), 21% with EC2 ($p < 0.05$), 15% with EC3 ($p < 0.05$), and 19% with EC4 ($p < 0.05$). By contrast, CS was approximately 4%, and N was 8%, both close to or below control. This indicates that ECs increased the proportion of adherent cells by approximately 2- to 2.3-fold relative to control, whereas CS and N did not. Adhesion markers were approximately 30% higher in adherent cells than in floating cells. All ECs slightly, but not significantly, elevated integrin CD11a above the control value in adherent cells. N lowered adherent-cell integrin CD11a expression ($p < 0.05$). For integrin CD11b, in floating cells, it increased significantly with

EC1 ($p < 0.05$) and CS ($p < 0.05$); EC4 also induced a rise, but the strongest effect was still moderate compared with adherent cells. In adherent cells, all EC aerosols and CS increased integrin CD11b, with the largest elevations seen for EC2 ($p < 0.01$) and EC4 ($p < 0.01$), both reaching highly significant levels. N did not significantly increase integrin CD11b expression in either floating or adherent cells.

CD54 rose significantly in floating cells only with EC1 ($p < 0.01$) and EC2 ($p < 0.05$) exposures, while in adherent cells, CD54 expression was generally higher than in floating cells, especially after EC3 ($p < 0.01$) and EC4 ($p < 0.05$). TNFα also showed clearer increases in adherent cells, especially with EC2 ($p < 0.01$), EC4 ($p < 0.01$), and CS ($p < 0.01$), where values were significantly above control.

EC aerosols and CS increased intracellular inflammation-related markers and DCF-associated oxidative fluorescence irrespective of cell adhesion status, with the strongest effects seen for adhering cells and CS and EC3/EC4 exposures. DCF-associated oxidative fluorescence in adherent cells exposed to EC3 and EC4 increased about twofold ($p < 0.01$), while N showed a different pattern, i.e., did not significantly alter oxidative stress in either floating or adherent cells.

In general, DCF-associated oxidative fluorescence increased significantly in all floating cells, with rather moderate increases after EC1 and EC2 (both $p < 0.05$) and higher increases after EC3 ($p < 0.01$) and EC4 ($p < 0.01$), and was the highest (more than 3-fold; $p < 0.01$) after CS. In adherent cells, the stress was even more elevated across EC1-EC4 (all $p < 0.01$), with almost a two-fold increase in EC3 ($p < 0.01$) and by about 3.5-fold ($p < 0.01$) with CS. N did not produce the same inflammatory/pro-oxidative pattern; it was not significant or near control in both floating and adherent cells.

Concerning inflammation, in floating cells, TNFα increased significantly after EC2 ($p < 0.05$), EC3 ($p < 0.05$), EC4 ($p < 0.05$) and CS ($p < 0.05$), but not with EC1. N decreased TNFα significantly only compared with the CS reference ($p < 0.01$). In adherent cells, TNFα was slightly higher across all EC treatments, especially with EC3 ($p < 0.05$) and EC4 ($p < 0.05$), and was highly increased with CS ($p < 0.01$), whereas N showed no significant effect.

Phagocytosis tended to decrease in floating cells, with significant reductions seen for EC4 ($p < 0.05$), CS ($p < 0.05$), and N ($p < 0.05$). In adherent cells, phagocytosis was less clearly affected and not significantly different from control.

3.3. Inflammation vs. Dcf-Associated Oxidative Fluorescence in Adherent and Nonadherent THP-1 Cells

Figures 2A–E and 3A–D and Table 2 present representative bivariate dot plots and quantitative results from dual-fluorescence analyses of floating and adherent THP-1 cells stained with the green oxidative-stress-sensitive probe H_2DCFDA and a red fluorescent anti-TNFα monoclonal antibody as a marker of inflammatory activation. Control and EC-exposed THP-1 cells were double-labelled, acquired on a Beckman Coulter CytoFLEX flow cytometer, and visualised as bivariate fluorescence density plots (Figure 2A,B), allowing assessment of the relationship between DCF-associated oxidative fluorescence in the green channel and TNF-α expression in the red channel in terms of cell population dispersion, distribution, and direction.

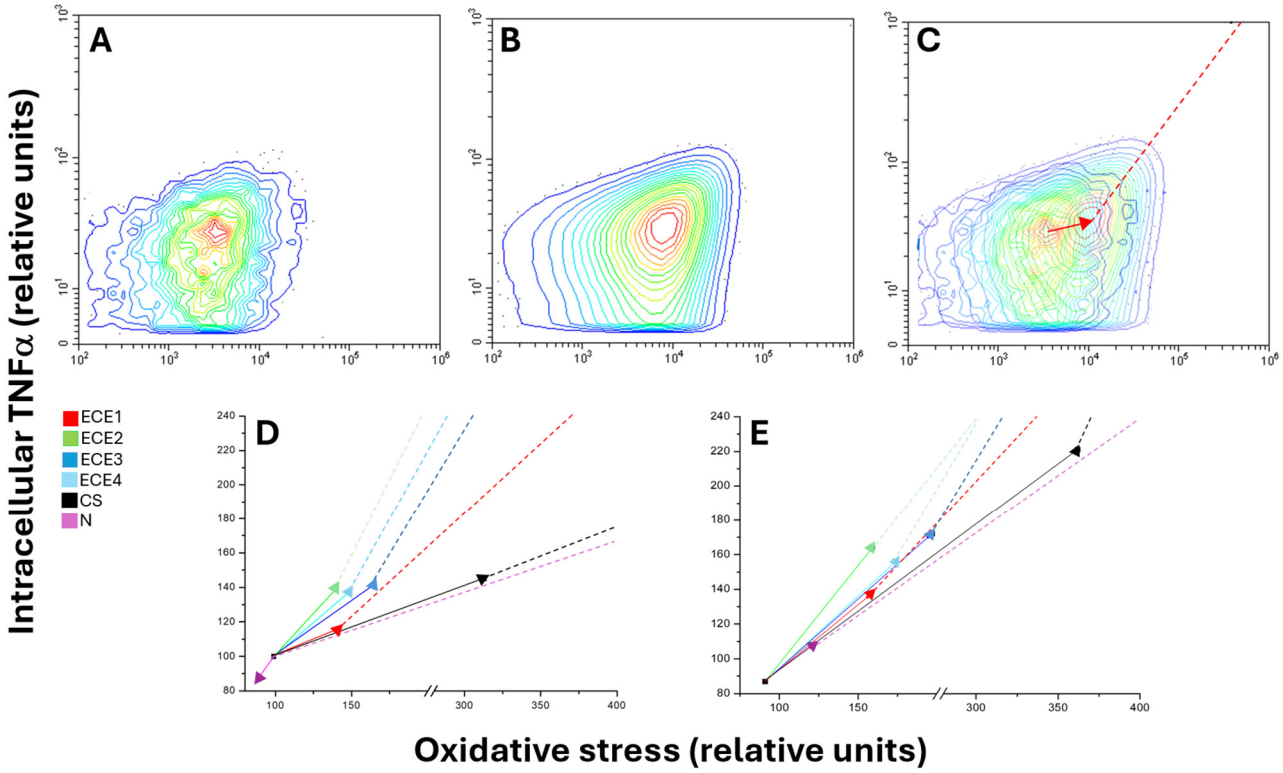


Figure 2. Representative scatterplots from double fluorescence experiments with the following: panel (**A**): control floating cells; panel (**B**): EC1-exposed floating cells; panel (**C**): overlay and vector; panel (**D**): floating-cell group comparison; panel (**E**): adherent-cell group comparison. THP-1 cells were stained with a green H_2DCFDA dye for oxidative stress and with a red fluorescent monoclonal antibody specific for TNF-α (inflammation). Panel (**A**) shows representative scatterplots of control, floating THP-1 cells, and B floating cells exposed to EC1. Panel (**C**) shows overlapping scatterplots (**A**,**B**) with a vector (red arrow represents the distance and slope of the scatterplot central density point in control cells to the corresponding density point in EC-exposed cells) and a central tendency line (slope of the dotted symmetry line from the central density point to the highest plot values). Panel (**D**) shows all group vectors and central tendency lines of floating THP-1 cells, while panel (**E**) shows similar plots in adherent cells.

Table 2. Quantification of dual fluorescence scatterplot data in non-adherent (F) and adherent (A) THP-1 cells exposed for 24 h to EC1 (classic tobacco), EC2 (menthol), EC3 (watermelon) or EC4 (strawberry), cigarette smoke (CS) or nicotine (N), followed by staining with the green fluorescent probe H_2DCFDA to visualise oxidative stress and a red fluorescent monoclonal antibody specific for TNFα to show inflammatory activation. The table shows bivariate slope descriptors: mean vector slopes and central tendency slopes as bivariate fluorescence density plots. All units are relative; samples were run in triplicate, and the experiment was repeated four to five times. Data are means ± SD.

Slopes of DCF-Associated Oxidative Fluorescence/TNF-α Vectors and Central Tendency Lines							
		EC1	EC2	EC3	EC4	CS	N
Vector slope	F	0.45 ± 0.13 $^{\wedge\wedge''}$	0.73 ± 0.16 $^{\wedge\wedge''}$	1.11 ± 0.18 $^{\wedge\wedge''}$	0.87 ± 0.17 $^{\wedge\wedge''}$	0.38 ± 0.18 $^{''}$	1.88 ± 0.19 $^{\wedge\wedge}$
	A	0.90 ± 0.15 $^{\#\#}$	0.93 ± 0.16	1.33 ± 0.17 $^{\wedge\wedge}$	0.97 ± 0.14 $^{\wedge}$	0.75 ± 0.17 $^{\#\#}$	0.78 ± 0.15 $^{\#\#}$
Slope of central tendency line	F	0.78 ± 0.16 $^{\wedge\wedge''++}$	1.19 ± 0.20 $^{\wedge\wedge''++}$	1.43 ± 0.16 $^{\wedge\wedge''++}$	1.38 ± 0.21 $^{\wedge\wedge''++}$	0.40 ± 0.19 $^{''}$	1.89 ± 0.23 $^{++}$
	A	0.93 ± 0.19 $^{\wedge\wedge''}$	1.66 ± 0.18 $^{\#\#''++}$	1.38 ± 0.15 $^{''}$	1.23 ± 0.18 $^{\#''+}$	1.48 ± 0.22 $^{\#\#''++}$	0.32 ± 0.14 $^{\#\#++}$

$^{\#}$ $p < 0.05$; $^{\#\#}$ $p < 0.01$ for comparisons between control floating cells subjected to the same treatment; $^{\wedge}$ $p < 0.05$; $^{\wedge\wedge}$ $p < 0.01$ for comparisons with CS-treated cells; $^{''}$ $p < 0.01$ for comparisons with N-treated cells; $^{+}$ $p < 0.05$; $^{++}$ $p < 0.01$ for comparisons with the corresponding vector slopes.

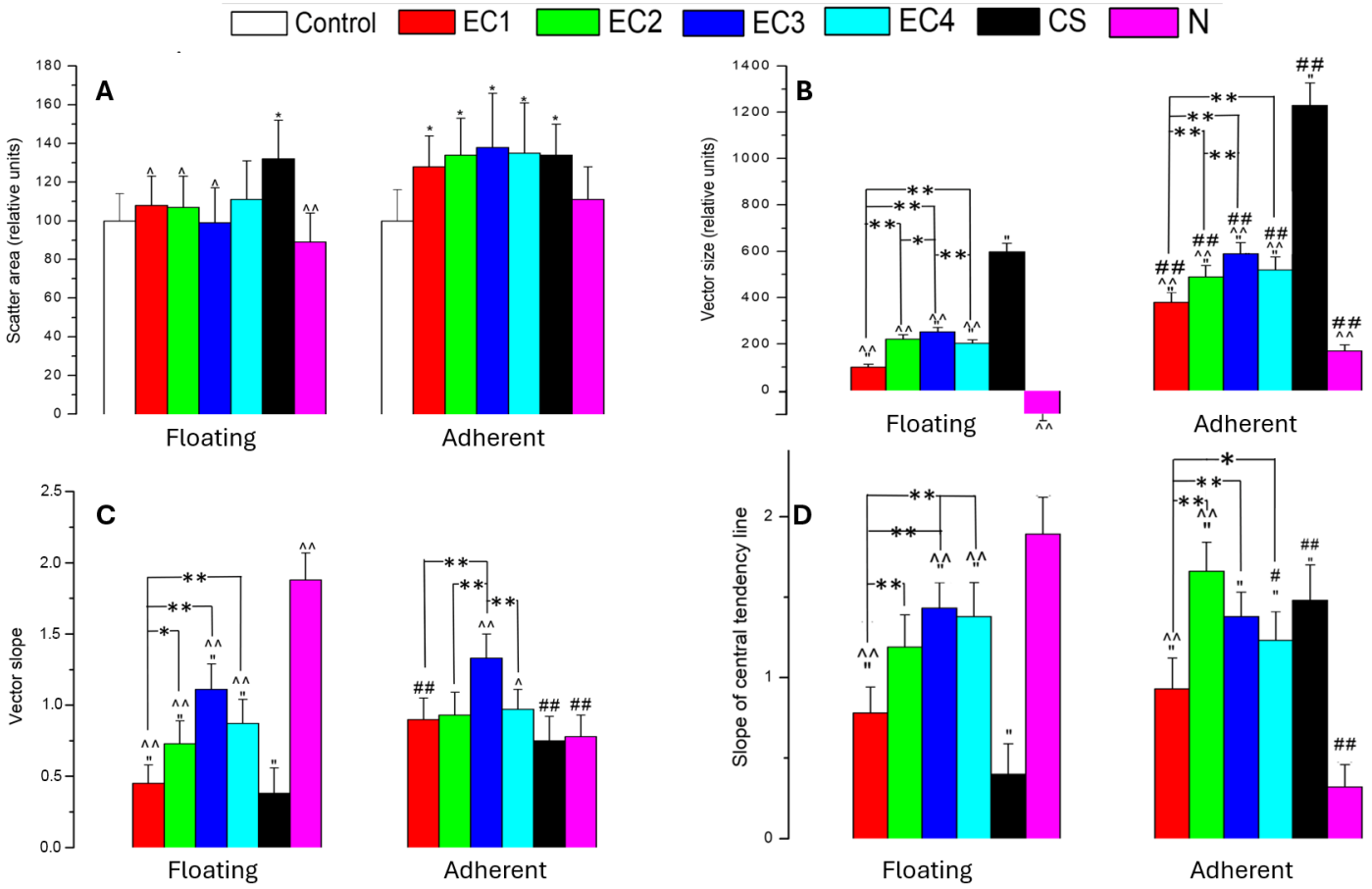


Figure 3. Quantification of dual-fluorescence scatterplot data in non-adherent and adherent THP-1 cells exposed for 24 h to EC1 (classic tobacco), EC2 (menthol), EC3 (watermelon), EC4 (strawberry), cigarette smoke (CS) or nicotine (N), followed by staining with the green fluorescent probe H_2DCFDA to visualise oxidative stress and a red fluorescent monoclonal antibody specific for TNF-α to show inflammatory activation. We plotted experimental data as bivariate fluorescence density plots and further analysed the scatter area (**A**), vector slope (**B**), vector distance from the control density point to the treatment-specific density point (**C**), and central-tendency slope (**D**). Table 2 shows statistical analyses of vector slopes and symmetry line slopes. All units are relative; samples were run in triplicate, and the experiment was repeated five times. Data are means ± SD. * $p < 0.05$; ** $p < 0.01$ for comparisons with the corresponding control cells or significance bracket for two EC bars; # $p < 0.05$; ## $p < 0.01$ for comparisons between control floating cells subjected to the same treatment; ^ $p < 0.05$; ^^ $p < 0.01$ for comparisons with CS-treated cells; '' $p < 0.01$ for comparisons with N-treated cells.

In floating cells, scatter area (Figure 3A) did not change after exposure to EC1, EC2, EC3, or EC4, but increased significantly ($p < 0.05$) after cigarette smoke, whereas N had no effect. In adherent cells (Figure 3A), scatter area slightly increased after EC3, EC4, and CS ($p < 0.05$ for all groups) but again not after nicotine.

Vector size in floating cells (Figure 3B) increased after EC2 and EC3, and EC4, peaked after CS (both $p < 0.01$ vs. EC1), and decreased sharply after N ($p < 0.01$), indicating that the redox–inflammatory displacement was not uniform across exposures. In adherent cells (Figure 3B), the changes were even greater, particularly after EC3, EC4, and CS ($p < 0.01$), while CS produced higher values, approximately two times more ($p < 0.01$) than in floating cells. Interestingly, N produced a vector in the opposite direction in adherent cells compared with floating cells.

The vector slope in floating cells (Figure 3C, and Table 2) varied significantly from 0.45 in EC1-treated cells to 1.11 for the EC3 group ($p < 0.01$) and to 0.87 ($p < 0.01$) for EC4-

treated cells; it was numerically similar to EC1 after CS, which has by far the largest vector value, but decreased vs. EC3-EC4 ($p < 0.05$) and increased after N ($p < 0.01$), compared to EC1-EC4.

In adherent cells (Figure 3C and Table 2), vector slopes were higher than in floating cells following EC1–EC4 and CS exposure, although the magnitude of this difference varied considerably between treatments. The largest relative increases were observed for EC1 (0.90 vs. 0.45; $p < 0.01$) and CS (0.75 vs. 0.38), whereas only modest increases were observed for EC2–EC4. In contrast, N produced the opposite pattern, with a lower vector slope in adherent than in floating cells (0.78 vs. 1.88; $p < 0.01$).

The slopes of the central tendency lines (Figure 3D, Table 2) were consistently steeper than the vector slopes in floating cells treated with EC1-EC4 and re-inverted after nicotine, supporting the idea that the balance between DCF-associated oxidative fluorescence and inflammation shifted away from a simple proportional pattern. The steepness of the central tendency line did not change in floating THP-1 cells treated with CS. In adherent cells, slope values were generally lower than in floating cells but commonly higher than the corresponding vector slopes. The central tendency slope again differed from the vector slope, especially for EC2 and CS, where it exceeded the vector slope, suggesting a marked rise in inflammation over DCF-associated oxidative fluorescence.

Overall, dual-fluorescence scatterplot analysis showed exposure-dependent remodelling of the relationship between DCF-associated oxidative fluorescence and TNF-α-related inflammation in THP-1 cells exposed to EC, CS or nicotine. CS produced the strongest shift, especially in adherent cells, with the largest vector size and the greatest divergence between vector slope and central-tendency slope, indicating uncoupling of redox and inflammatory responses. EC exposures caused intermediate changes, whereas N showed a tendency toward lower TNF-α and DCF-associated oxidative fluorescence values in floating cells and toward higher values in adherent cells, although these changes were generally not statistically significant. N appeared to exert antioxidant and anti-inflammatory effects in non-adherent cells, while in adherent cells, it showed a tendency toward pro-oxidant/pro-inflammatory behaviour, though generally weaker than CS and ECs.

4. Discussion

ECs are widely used as alternatives to conventional cigarettes, and their use has increased substantially in recent years [22]. E-liquids typically contain propylene glycol and/or vegetable glycerin as base solvents, together with flavouring compounds and, in many products, N at concentrations that may reach 48 mg/mL [23]. A growing body of evidence indicates that EC exposure can induce a range of biological effects in cellular, animal, and human studies [3,4,24]. The present findings indicate that exposure of THP-1 cells to the EC aerosol-conditioned media elicited measurable biological responses, although these were generally less pronounced than those induced by CS-conditioned medium. The clearest difference was observed for acute cytotoxicity: CS-conditioned medium substantially increased cell death, membrane damage, and the sub-G1 DNA fraction, whereas EC-conditioned media and N alone produced considerably smaller effects. These findings are consistent with previous observations [25,26] and indicate that the tested EC formulations are not biologically inert, although they produced substantially less acute cytotoxicity than cigarette smoke under the present experimental conditions. Importantly, the absence of pronounced cytotoxicity should not be interpreted as an absence of biological activity. Clear functional differences between experimental groups were observed, especially in cell adhesion and in the expression of adhesion-related proteins. CD11a, CD11b, and CD54 are cell-surface adhesion molecules involved in leukocyte adhesion, migration, and inflammatory responses [27,28]. EC exposure increased the proportion of adherent cells and was

associated with formulation- and subpopulation-dependent changes in CD11a, CD11b, and CD54 expression, with the most pronounced responses generally observed in adherent cells. This study cannot determine whether increased adherence preceded the marker changes, followed them, or reflected preferential retention of cells with particular phenotypic characteristics but the described pattern may be consistent with a shift toward a more activated cellular phenotype characterised by increased adhesive properties. Such changes may be biologically relevant, as monocyte activation and adhesion are recognised features of inflammatory responses and have been implicated in vascular inflammation [29]. Together with the observed changes in TNF-α expression and oxidative activity, increased adhesion after EC exposure is consistent with a shift toward a pro-inflammatory cellular phenotype, despite the absence of substantial cytotoxicity. The responses also varied among formulations; menthol produced the greatest increase in the adherent-cell fraction, whereas watermelon and strawberry were associated with the largest increases in oxidative activity and less consistently with TNF-α expression, particularly within the adherent subpopulation.

Oxidative response data further support the presence of formulation- and cell-subpopulation-dependent effects. EC exposure increased DCF-associated fluorescence, particularly in adherent cells, with the largest increases observed for the watermelon and strawberry flavours. The watermelon and strawberry preparations also showed relatively high numerical responses for selected endpoints.

Previous studies have shown that fruit- and sweet-flavoured EC formulations can induce pronounced oxidative responses in airway epithelial cells, while selected flavouring constituents can also impair mitochondrial function [30–32].

N alone did not significantly alter DCF-associated oxidative fluorescence or intracellular TNF-α-associated fluorescence relative to the corresponding controls. Numerical differences between adherent and nonadherent fractions remain exploratory and do not demonstrate opposing biological activities. However, this finding may be significant, as it demonstrates that EC safety cannot be assessed solely based on N content. Of particular interest, N exhibited opposing anti-inflammatory and antioxidant effects in adherent THP-1 cells compared with their nonadherent (floating) counterparts. N is recognised as having a dual role in inflammation: It may act as an immunosuppressant and anti-inflammatory mediator by engaging α7 nicotinic acetylcholine receptors (α7-nAChRs) on THP-1 cells, leading to suppression of pro-inflammatory cytokines, including TNF-α [33,34]. However, depending on cell type, concentration, and exposure duration, N can also either exacerbate or mitigate oxidative stress [35,36]. These context-dependent effects underscore the need for further mechanistic studies to clarify the nature of N interactions within EC aerosol exposures.

TNFα expression also increased following exposure, with generally greater responses in adherent than in nonadherent cells. The greater TNF-α response observed in adherent cells is consistent with an association between the adherent phenotype and enhanced inflammatory activation. TNF-α is a key pro-inflammatory cytokine produced by activated monocytes, macrophages, and other immune cells [37]. It promotes inflammation by activating endothelial cells, increasing vascular permeability, and recruiting neutrophils and other leukocytes to sites of infection or tissue injury [38,39]. Although TNF-α is essential for host defence, excessive or prolonged TNF-α signalling can contribute to chronic inflammation and autoimmune disease [39]. Previous studies have reported higher levels of inflammatory markers, including IL-6 and TNF-α, in EC users than in non-smokers, although these levels were generally lower than those observed in cigarette smokers [40,41]. This finding is consistent with the concept that cell adhesion is associated with a more pro-inflammatory phenotype [42]. The largest increases in TNF-α expression were observed following exposure to selected flavoured EC formulations and CS, suggesting that individual e-liquid formulations differ in their capacity to induce inflammatory cellular responses

despite producing less acute cytotoxicity than CS. Together, these findings further support formulation-dependent differences in EC-induced cellular responses.

Bivariate analysis of DCF-associated oxidative fluorescence and TNF-α expression provided additional information on the distribution of cellular responses. We previously demonstrated that bivariate fluorescence scatterplot analysis can reveal exposure-specific changes within heterogeneous mononuclear cell populations that may not be fully captured by conventional single-parameter analyses [43]. Scatterplot analysis showed that aerosol exposure affected not only the magnitude of individual responses but also the joint distribution of DCF-associated oxidative fluorescence and TNF-α expression within the cell population, a feature that may be obscured when only group-level averages are considered. The scatterplots therefore provide a complementary representation of aerosol-associated cellular responses, revealing both population heterogeneity and formulation-dependent differences. The bivariate analysis was also consistent with generally greater responses in adherent than in nonadherent cells. CS produced the largest overall shifts, whereas EC-induced changes were generally smaller and varied among formulations. This pattern suggests substantial cellular heterogeneity, with a subset of cells showing particularly pronounced DCF-associated oxidative fluorescence and inflammatory responses. The presence of a more strongly activated cellular subpopulation may warrant further investigation in models of repeated or chronic exposure.

Reduced phagocytic activity in selected groups may also have functional implications. Phagocytosis is a key defence mechanism of monocytes and macrophages, and its impairment may limit the clearance of foreign particles, cellular debris, and potentially toxic material. Previous studies have reported impaired phagocytic activity and increased production of pro-inflammatory cytokines, including IL-6, IL-8, and TNF-α, in human alveolar macrophages following exposure to EC vapour condensate [44,45]. Such alterations in macrophage function have been associated with impaired antimicrobial defence and increased susceptibility to respiratory infections [45,46]. Together with changes in adhesion, oxidative activity, and TNF-α expression, the observed reduction in phagocytosis in selected groups suggests that EC exposure may affect both activation-related markers and selected cellular functions under the present experimental conditions. Although the tested EC formulations produced substantially less acute cytotoxicity than CS under the present experimental conditions, they were not biologically inert.

In summary, the tested EC formulations induced pro-inflammatory and pro-oxidative changes in THP-1 cells, although these responses were generally less pronounced than those observed after CS exposure. Importantly, the magnitude and pattern of these responses varied among formulations, and N alone did not reproduce the overall response profile observed with the EC aerosol-conditioned media. Indirect exposure through a processed conditioned medium and the absence of aerosolised vehicles and N-free formulation controls prevent clear separation of the contributions of PG/VG, flavourings, and thermal degradation products. The inability to separate their interactions is the main limitation of our study. Despite the inherent limitations of an in vitro cell-line model, these findings indicate that the tested EC aerosols can induce an activated, pro-inflammatory and pro-oxidative phenotype in THP-1 cells under the present experimental conditions. Accordingly, the tested EC formulations exhibited measurable biological activity, and their inflammatory, oxidative, and functional effects warrant further investigation in repeated- and chronic-exposure models. This study provides an integrated in vitro approach for comparing the oxidative, inflammatory, and functional effects of different EC aerosol formulations and supports further evaluation of THP-1-based models for comparative toxicological screening. Future studies should determine whether these exposure-specific

cellular response patterns are reproducible in primary human cells and more physiologically relevant experimental models.

Author Contributions: Conceptualization, K.M. and A.H.; methodology, K.M., P.S., J.R. and A.H.; software, P.S. and K.M.; validation, K.M., A.H. and J.R.; formal analysis, A.H.; investigation, K.M.; resources, A.H.; data curation, K.M.; writing—original draft preparation, K.M.; writing—review and editing, A.H.; visualization, K.M.; supervision, A.H.; project administration, K.M. and A.H.; funding acquisition, A.H. All authors have read and agreed to the published version of the manuscript.

Funding: This research received external funding from the Medical University of Bialystok. Grant number B.SUB.25.385.

Institutional Review Board Statement: Not applicable.

Informed Consent Statement: Not applicable.

Data Availability Statement: The data presented in this study are available from the corresponding author upon reasonable request.

Conflicts of Interest: The authors declare no conflicts of interest.

References

1. Liu, T.; Loo, L.W.M.; Huang, B.Z.; Quon, B.; Guillermo, C.; Siegmund, K.D.; Wilkens, L.R.; Maunakea, A.K.; Hecht, S.S.; Murphy, S.E.; et al. The association of epigenetic age acceleration with internal smoking dose, risk of lung cancer, and all-cause mortality in cigarette smokers: The Multiethnic Cohort study. *Clin. Epigenet.* **2026**, *18*, 110. [CrossRef] [PubMed] [PubMed Central]
2. Fenercioglu, A.K.; Uzun, H.; Unal, D.O. The Convergent Immunopathogenesis of Cigarette Smoke Exposure: From Oxidative Stress to Epigenetic Reprogramming in Chronic Disease. *Int. J. Mol. Sci.* **2025**, *27*, 187. [CrossRef] [PubMed] [PubMed Central]
3. Manchen, P.J.; Larsen, B.T.; Smith, M.L.; Tazelaar, H.D.; Butt, Y.M. EVALI and Beyond: An Update on the Spectrum of Vaping-Associated Lung Pathology. *Am. J. Surg. Pathol.* **2026**, *50*, 1231–1239. [CrossRef] [PubMed]
4. Kimbrough, M.; Cius, E. Electronic Cigarettes: A Comprehensive Review for Primary Care Providers. *Prim. Care Clin. Off. Pract.* **2026**, *53*, 371–385. [CrossRef] [PubMed]
5. Tareq, M.M.I.; Nair, S.; He, G. Emerging multisystem disease mechanisms of e-cigarette vaping on human health. *Toxicol. Rep.* **2026**, *16*, 102282. [CrossRef] [PubMed] [PubMed Central]
6. Vázquez-López, N.I.; Falfán-Valencia, R.; Pérez-Rubio, G. Findings on e-cigarette flavors and their implications for human health: A systematic review. *Front. Public Health* **2026**, *14*, 1807715. [CrossRef] [PubMed] [PubMed Central]
7. Rahimi, H.; Hong, J.; Maldonado Zimbron, V.; Phillips, A.; Burrowes, K. Structural and molecular alterations in lung lymphatic endothelial cells induced by cigarette smoking: Insights and emerging hypotheses for vaping. *Am. J. Physiol. Lung Cell. Mol. Physiol.* **2026**, *330*, L634–L652. [CrossRef] [PubMed]
8. Sailis, A.B. Ferroptosis in e-cigarette aerosol-associated respiratory injury. *Arch. Toxicol.* **2026**, *100*, 5247–5260. [CrossRef] [PubMed]
9. Limanaqi, F.; Zecchini, S.; Ogno, P.; Artusa, V.; Fenizia, C.; Saulle, I.; Vanetti, C.; Garziano, M.; Strizzi, S.; Trabattoni, D.; et al. Alpha-synuclein shapes monocyte and macrophage cell biology and functions by bridging alterations of autophagy and inflammatory pathways. *Front. Cell Dev. Biol.* **2024**, *12*, 1421360. [CrossRef] [PubMed] [PubMed Central]
10. Anderson, C.; Majeste, A.; Hanus, J.; Wang, S. E-Cigarette Aerosol Exposure Induces Reactive Oxygen Species, DNA Damage, and Cell Death in Vascular Endothelial Cells. *Toxicol. Sci.* **2016**, *154*, 332–340. [CrossRef] [PubMed]
11. Wang, H.; Tian, Y.; Li, S.; Li, P.; Geng, N.; Li, X.; Cui, L.; Fu, Y.; Han, S.; Chen, H.; et al. Multi-endpoint in vitro toxicity profiling of heated tobacco products versus e-cigarettes under air-liquid interface exposure. *Toxicol. In Vitro* **2026**, *116*, 106267. [CrossRef] [PubMed]
12. Sompa, S.I.; Upadhyay, S.; Ganguly, K.; Bergström, A.; Ji, J.; Palmberg, L. Epithelial effects of exposure to e-cigarettes alone or in combination with cigarette smoke using multicellular lung mucosa models. *Environ. Toxicol. Pharmacol.* **2026**, *124*, 104989. [CrossRef] [PubMed]
13. Spurrier-Best, L.; Butcher, D.; Blackham-Hayward, E.; Kertesz, Z.; Chichger, H. Nicotine-free electronic vape fluid stimulates angiogenic processes in vitro through ARF6-mediated oxidative stress. *Front. Toxicol.* **2026**, *7*, 1699112. [CrossRef] [PubMed] [PubMed Central]
14. Sutkowy, P.; Hadryś, I.; Gmys, W.; Grzempa, P.; Sobieszczańska, A.; Tuska, W.; Błachnio, K.; Woźniak, A. Molecular Health Effects of Electronic Cigarettes. *Biomolecules* **2026**, *16*, 264. [CrossRef] [PubMed] [PubMed Central]

15. Wawryk-Gawda, E.; Zarobkiewicz, M.K.; Wolanin-Stachyra, M.; Opoka-Winiarska, V. Inflammatory markers activation associated with vapor or smoke exposure in Wistar rats. *Front. Immunol.* **2025**, *16*, 1525166. [CrossRef] [PubMed] [PubMed Central]
16. Beigh, S.; Jawed, A.; Dar, S.A. Beyond Nicotine: Toxicological Insights Into Metals, Nanoparticles, and Flavoring Agents in E-Cigarette Aerosols. *J. Appl. Toxicol.* **2026**. [CrossRef] [PubMed]
17. Roslan, M.; Milewska, K.; Szoka, P.; Warpechowski, K.; Borawski, K.; Milewski, J.; Holownia, A. Selective Activation of Human Monocytes Exposed Ex Vivo to Different E-Cigarette Aerosols: Possible Role in Subclinical Inflammation. *Cells* **2026**, *15*, 397. [CrossRef] [PubMed] [PubMed Central]
18. Roslan, M.; Milewska, K.; Szoka, P.; Warpechowski, K.; Milkowska, U.; Holownia, A. Diverse Impact of E-Cigarette Aerosols on Oxidative Stress and Inflammation in Lung Alveolar Epithelial Cells (A549). *Int. J. Mol. Sci.* **2025**, *26*, 10967. [CrossRef] [PubMed] [PubMed Central]
19. Shipman, J.G.; Mundy, K.; Onyenwoke, R.U.; Sivaraman, V. Vaping induces a marked pro-inflammatory state within the lung, which is at least partially due to its immunomodulatory effects. *Front. Immunol.* **2026**, *17*, 1759361. [CrossRef] [PubMed] [PubMed Central]
20. Testa, M.P.; Alvarado, O.; Wournell, A.; Lee, J.; Guilford, F.T.; Henriksen, S.H.; Phillips, T.R. Screening assay for oxidative stress in a feline astrocyte cell line, G355-5. *J. Vis. Exp.* **2011**, *53*, e2841. [CrossRef] [PubMed] [PubMed Central]
21. Daigneault, M.; Preston, J.A.; Marriott, H.M.; Whyte, M.K.; Dockrell, D.H. The identification of markers of macrophage differentiation in PMA-stimulated THP-1 cells and monocyte-derived macrophages. *PLoS ONE* **2010**, *5*, e8668. [CrossRef] [PubMed] [PubMed Central]
22. Sissung, T.M.; Figg, W.D. Commentary: Electronic Nicotine Delivery Systems: Seeing Through the Clouds. *Fam. Community Health* **2022**, *45*, 202–205. [CrossRef] [PubMed] [PubMed Central]
23. Ween, M.P.; Moshensky, A.; Thredgold, L.; Bastian, N.A.; Hamon, R.; Badiei, A.; Nguyen, P.T.; Herewane, K.; Jersmann, H.; Bojanowski, C.M.; et al. E-cigarettes and health risks: More to the flavor than just the name. *Am. J. Physiol. Lung Cell. Mol. Physiol.* **2021**, *320*, L600–L614. [CrossRef] [PubMed] [PubMed Central]
24. Ward, A.M.; Yaman, R.; Ebbert, J.O. Electronic nicotine delivery system design and aerosol toxicants: A systematic review. *PLoS ONE* **2020**, *15*, e0234189. [CrossRef] [PubMed] [PubMed Central]
25. Li, X.; Tian, Y.; Wang, H.; Jiang, Y.; Chen, Y.; Han, S.; Song, Z.; Cui, L.; Chen, H.; Hou, H. Divergent mechanisms of menthol and tobacco e-cigarette toxicity in a 3D airway organoid model: Metabolic disruption and immunosuppression versus Th2-Allergic inflammation and apoptotic stress. *Chem. Biol. Interact.* **2026**, *434*, 112121. [CrossRef] [PubMed]
26. Guraka, A.; Mierlea, S.; Drake, S.J.; Shawa, I.T.; Waldron, J.; Corcoran, M.; Dowse, D.; Walkman, D.; Burn, L.; Sivasubramaniam, S.; et al. A comprehensive toxicological analysis of panel of unregulated e-cigarettes to human health. *Toxicology* **2024**, *509*, 153964. [CrossRef] [PubMed]
27. Li, M.J.; Cui, F.M.; Cheng, Y.; Sun, D.; Zhou, P.K.; Min, R. Changes in the adhesion and migration ability of peripheral blood cells: Potential biomarkers indicating exposure dose. *Health Phys.* **2014**, *107*, 242–247. [CrossRef] [PubMed]
28. Ley, K.; Laudanna, C.; Cybulsky, M.I.; Nourshargh, S. Getting to the site of inflammation: The leukocyte adhesion cascade updated. *Nat. Rev. Immunol.* **2007**, *7*, 678–689. [CrossRef] [PubMed]
29. Xu, K.; Saaoud, F.; Yu, S.; Drummer, C., 4th; Shao, Y.; Sun, Y.; Lu, Y.; Sun, J.; Yu, J.; Jiang, X.; et al. Monocyte Adhesion Assays for Detecting Endothelial Cell Activation in Vascular Inflammation and Atherosclerosis. In *Methods in Molecular Biology*; Humana: New York, NY, USA, 2022; Volume 2419, pp. 169–182. [CrossRef] [PubMed] [PubMed Central]
30. Muthumalage, T.; Lamb, T.; Friedman, M.R.; Rahman, I. E-cigarette flavored pods induce inflammation, epithelial barrier dysfunction, and DNA damage in lung epithelial cells and monocytes. *Sci. Rep.* **2019**, *9*, 19035. [CrossRef] [PubMed] [PubMed Central]
31. Jabba, S.V.; Diaz, A.N.; Erythropel, H.C.; Zimmerman, J.B.; Jordt, S.E. Chemical Adducts of Reactive Flavor Aldehydes Formed in E-Cigarette Liquids Are Cytotoxic and Inhibit Mitochondrial Function in Respiratory Epithelial Cells. *Nicotine Tob. Res.* **2020**, *22*, S25–S34. [CrossRef] [PubMed] [PubMed Central]
32. Lerner, C.A.; Sundar, I.K.; Yao, H.; Gerloff, J.; Ossip, D.J.; McIntosh, S.; Robinson, R.; Rahman, I. Vapors produced by electronic cigarettes and e-juices with flavorings induce toxicity, oxidative stress, and inflammatory response in lung epithelial cells and in mouse lung. *PLoS ONE* **2015**, *10*, e0116732. [CrossRef] [PubMed] [PubMed Central]
33. Pavlov, V.A.; Tracey, K.J. The cholinergic anti-inflammatory pathway. *Brain Behav. Immun.* **2005**, *19*, 493–499. [CrossRef] [PubMed]
34. Yoshikawa, H.; Kurokawa, M.; Ozaki, N.; Nara, K.; Atou, K.; Takada, E.; Kamochi, H.; Suzuki, N. Nicotine inhibits the production of proinflammatory mediators in human monocytes by suppression of I-kappaB phosphorylation and nuclear factor-kappaB transcriptional activity through nicotinic acetylcholine receptor alpha7. *Clin. Exp. Immunol.* **2006**, *146*, 116–123. [CrossRef] [PubMed] [PubMed Central]
35. Soto-Otero, R.; Méndez-Alvarez, E.; Hermida-Ameijeiras, A.; López-Real, A.M.; Labandeira-García, J.L. Effects of (-)-nicotine and (-)-cotinine on 6-hydroxydopamine-induced oxidative stress and neurotoxicity: Relevance for Parkinson's disease. *Biochem. Pharmacol.* **2002**, *64*, 125–135. [CrossRef] [PubMed]

36. Morosini, C.; Vivarelli, F.; Paolini, M.; Canistro, D. Heated Tobacco Products: Emerging Health Outcomes and Insights into Oxidative Stress and Pro-Inflammatory-Driving Mechanisms. *Antioxidants* **2025**, *15*, 8. [CrossRef] [PubMed] [PubMed Central]
37. Jang, D.I.; Lee, A.H.; Shin, H.Y.; Song, H.R.; Park, J.H.; Kang, T.B.; Lee, S.R.; Yang, S.H. The Role of Tumor Necrosis Factor Alpha (TNFα) in Autoimmune Disease and Current TNFα Inhibitors in Therapeutics. *Int. J. Mol. Sci.* **2021**, *22*, 2719. [CrossRef] [PubMed] [PubMed Central]
38. Akbarzadeh, R.; Beerens, M.; Humrich, J.Y.; Kusche, K.; Lamprecht, P.; Riemekasten, G.; Renné, T. Role of neutrophils in regulating vascular permeability in inflammatory and autoimmune diseases. *Inflamm. Res.* **2026**, *75*, 35. [CrossRef] [PubMed] [PubMed Central]
39. Yu, K.; Yu, C.; Jiao, L.; Miao, K.; Ni, L.; Rao, X.; Zhou, L.; Zhao, C. The Function and Therapeutic Implications of TNF Signaling in MDSCs. *Biomolecules* **2022**, *12*, 1627. [CrossRef] [PubMed] [PubMed Central]
40. Billa, A.L.; Sukhabogi, J.R.; Doshi, D.; Athe, R. Systemic and Salivary Cytokine Levels among Adult E-Cigarette Users: A Systematic Review and Meta Analysis. *Asian Pac. J. Cancer Prev.* **2025**, *26*, 2327–2338. [CrossRef] [PubMed] [PubMed Central]
41. Boakye, E.; Uddin, S.M.I.; Osuji, N.; Meinert, J.; Obisesan, O.H.; Mirbolouk, M.; Tasdighi, E.; El-Shahawy, O.; Erhabor, J.; Osei, A.D.; et al. Examining the association of habitual e-cigarette use with inflammation and endothelial dysfunction in young adults: The VAPORS-Endothelial function study. *Tob. Induc. Dis.* **2023**, *21*, 75. [CrossRef] [PubMed] [PubMed Central]
42. Block, A.; Liu, X.; Zhang, D.; Adebowale, K. Engineering macrophages for cancer immunotherapy: Emerging insights and therapeutic potential. *npj BioMed. Innov.* **2026**, *3*, 18. [CrossRef] [PubMed] [PubMed Central]
43. Niechoda, A.; Roslan, M.; Milewska, K.; Szoka, P.; Maciorowska, K.; Holownia, A. Signalling Pathways of Inflammation and Cancer in Human Mononuclear Cells: Effect of Nanoparticle Air Pollutants. *Cells* **2024**, *13*, 1367. [CrossRef] [PubMed] [PubMed Central]
44. Scott, A.; Lugg, S.T.; Aldridge, K.; Lewis, K.E.; Bowden, A.; Mahida, R.Y.; Grudzinska, F.S.; Dosanjh, D.; Parekh, D.; Foronjy, R.; et al. Pro-inflammatory effects of e-cigarette vapour condensate on human alveolar macrophages. *Thorax* **2018**, *73*, 1161–1169. [CrossRef] [PubMed] [PubMed Central]
45. Sniadach, J.; Kicman, A.; Michalska-Falkowska, A.; Jonczyk, K.; Waszkiewicz, N. Changes in Concentration of Selected Biomarkers of Exposure in Users of Classic Cigarettes, E-Cigarettes, and Heated Tobacco Products—A Narrative Review. *Int. J. Mol. Sci.* **2025**, *26*, 1796. [CrossRef] [PubMed] [PubMed Central]
46. Corriden, R.; Moshensky, A.; Bojanowski, C.M.; Meier, A.; Chien, J.; Nelson, R.K.; Crotty Alexander, L.E. E-cigarette use increases susceptibility to bacterial infection by impairment of human neutrophil chemotaxis, phagocytosis, and NET formation. *Am. J. Physiol. Cell Physiol.* **2020**, *318*, C205–C214. [CrossRef] [PubMed] [PubMed Central]

Disclaimer/Publisher's Note: The statements, opinions and data contained in all publications are solely those of the individual author(s) and contributor(s) and not of MDPI and/or the editor(s). MDPI and/or the editor(s) disclaim responsibility for any injury to people or property resulting from any ideas, methods, instructions or products referred to in the content.